

Akito Kawai,^a Shigesada Higuchi,^a Masaru Tsunoda,^{b,c} Kazuo T. Nakamura^b and Shuichi Miyamoto^{a*}

^aFaculty of Pharmaceutical Sciences, Sojo University, 4-22-1 Ikeda, Kumamoto 860-0082, Japan, ^bSchool of Pharmacy, Showa University, 1-5-8 Hatanodai, Shinagawa-ku, Tokyo 142-8555, Japan, and ^cFaculty of Pharmacy, Iwaki Meisei University, Chuodai-iino, Iwaki 970-8551, Japan

Correspondence e-mail:
miyamoto@ph.soho-u.ac.jp

Received 16 September 2009
Accepted 26 October 2009

Purification, crystallization and preliminary X-ray analysis of the PCNA2–PCNA3 complex from *Sulfolobus tokodaii* strain 7

Crenarchaeal PCNA is known to consist of three subunits (PCNA1, PCNA2 and PCNA3) that form a heterotrimer (PCNA123). Recently, another heterotrimeric PCNA composed of only PCNA2 and PCNA3 was identified in *Sulfolobus tokodaii* strain 7 (stoPCNAs). In this study, the purified stoPCNA2–stoPCNA3 complex was crystallized by hanging-drop vapour diffusion. The crystals obtained belonged to the orthorhombic space groups $I222$ and $P2_12_12$, with unit-cell parameters $a = 91.1$, $b = 111.8$, $c = 170.9$ Å and $a = 91.1$, $b = 160.6$, $c = 116.6$ Å, respectively. X-ray diffraction data sets were collected to 2.90 Å resolution for the $I222$ crystals and to 2.80 Å resolution for the $P2_12_12$ crystals.

1. Introduction

DNA metabolism is mediated by protein complexes that consist of various DNA-processing proteins. The DNA sliding-clamp family of proteins interact with various DNA-processing proteins and play a central role as a platform for these proteins on DNA (for a review, see Moldovan *et al.*, 2007). The DNA sliding-clamp family consists of β -clamps in bacteria and proliferating cell nuclear antigens (PCNAs) in eukarya and archaea.

Crystal structures of DNA sliding clamps have been reported for *Escherichia coli* (Kong *et al.*, 1992), human (Gulbis *et al.*, 1996), *Saccharomyces cerevisiae* (Krishna *et al.*, 1994), *Pyrococcus furiosus* (Matsumiya *et al.*, 2001) and *Sulfolobus solfataricus* (Williams *et al.*, 2006). Various structural components are known; for example, the bacterial β -clamp forms a homodimer, eukaryotic PCNAs form homotrimers and both homotrimeric and heterotrimeric structures exist in archaea. Nevertheless, structural analysis of DNA sliding clamps has revealed that they all form similar ring-shaped structures. In addition, DNA sliding-clamp structures suggest that a positively charged central cavity formed by α -helices associates with DNA and that DNA sliding clamps can slide freely on DNA. The interdomain-connecting loop (IDCL), which generally interacts with the DNA-processing proteins through the main motif known as the PIP box, is located on the outer side of the DNA sliding clamp.

A PCNA-forming heterotrimer has been found in three crenarchaeal species [*Sulfolobus solfataricus* (*sso*PCNAs; Dionne *et al.*, 2003), *Aeropyrum pernix* (*ape*PCNAs; Imamura *et al.*, 2007) and *Sulfolobus tokodaii* strain 7 (*sto*PCNAs; Lu *et al.*, 2008)]. Biochemical studies of the subunit interactions and complex formation indicate that the interactions between these subunits (PCNA1, PCNA2 and PCNA3) vary depending on the species. In *S. solfataricus*, *sso*PCNA1 and *sso*PCNA2 first form a stable heterodimer and then recruit *sso*PCNA3. In *S. tokodaii*, *sto*PCNA3 interacts with the other subunits, while no interaction (or little affinity) is observed between *sto*PCNA1 and *sto*PCNA2. Similarly, in *A. pernix* *ape*PCNA2 interacts with the other subunits, while no interaction (or little affinity) is observed between *ape*PCNA1 and *ape*PCNA3. Interestingly, *sto*PCNA2–*sto*PCNA3 and *ape*PCNA2–*ape*PCNA3 are able to form a heterotrimer without the respective PCNA1s. Furthermore, the heterotrimer *sto*PCNA2–*sto*PCNA3 enhances the activity of Hjc and reduces the activity of Hjm and DNA ligase I like *sto*PCNA123 and the heterotrimer *ape*PCNA2–*ape*PCNA3 enhances the activities



© 2009 International Union of Crystallography
All rights reserved

of DNA polymerase, DNA ligase I and Fen1 like *ape*PCNA123. However, the detailed functional and structural differences between PCNA123 and PCNA2–PCNA3 remain to be clarified.

The present paper describes the purification, crystallization and preliminary X-ray analysis of the *sto*PCNA2–*sto*PCNA3 complex. A three-dimensional structural study of the PCNA2–PCNA3 complex is anticipated to be able to help in understanding the structural and functional differences between PCNA123 and PCNA2–PCNA3.

2. Methods

2.1. Protein expression and purification

Recombinant *sto*PCNA2 and *sto*PCNA3 proteins were individually overexpressed in *Escherichia coli* BL21 (DE3) using the pET expression system (Novagen). The transformant cells were grown to an OD_{600} of 0.6 at 310 K in Luria–Bertani broth and 20% (w/v) lactose solution was added to give a final concentration of 1 mM. The cultures were grown for 4 h at 310 K and harvested by centrifugation (6500g for 20 min). The cells were resuspended in 20 mM Tris–HCl pH 8.0 and disrupted by sonication followed by incubation at 343 K for 30 min. After centrifugation (7000g for 30 min), ammonium sulfate was added to the supernatant to 45% saturation. After gentle stirring for 1 h at 277 K, the suspension was centrifuged (18 000g for 30 min) and ammonium sulfate was once again added to the supernatant to 65% saturation. After gentle stirring for 1 h at 277 K, the suspension was centrifuged (18 000g for 1 h) and the supernatant was removed. The precipitants were dissolved in 20 mM Tris–HCl pH 8.0 and the solution was dialyzed overnight against 11.20 mM Tris–HCl pH 8.0. Further purification was performed on a HiTrap Q anion-exchange column (GE Healthcare); the proteins were eluted using a linear gradient from 0 to 0.5 M NaCl in 20 mM Tris–HCl pH 8.0. The fractions containing *sto*PCNA as judged by SDS–PAGE analysis were dialyzed overnight against 11.20 mM Tris–HCl pH 8.0 and concentrated. The *sto*PCNA2–*sto*PCNA3 complex was formed by incubating the proteins in an equal molar ratio at 277 K overnight and was purified by gel filtration on a Superdex 75 pg column (GE Healthcare) in 20 mM Tris–HCl pH 8.0 containing 150 mM NaCl. The peak fractions containing the *sto*PCNA2–*sto*PCNA3 complex were collected and concentrated to 40 mg ml^{−1} for crystallization trials.

2.2. Crystallization

Initial crystallization screening of the *sto*PCNA2–*sto*PCNA3 complex was performed by the sitting-drop vapour-diffusion method using the Index, Crystal Screen and Crystal Screen 2 crystal screening kits (Hampton Research). Equal volumes (1.2 μ l) of protein solution and reservoir solution were mixed and the mixture was equilibrated against 0.1 ml reservoir solution in a 96-well sitting-drop Crystal-Quick plate (Greiner Bio-One). The crystallization conditions were optimized using the hanging-drop vapour-diffusion method by mixing 1.5 μ l protein solution and 1.5 μ l reservoir solution and equilibrating this mixture against 1 ml reservoir solution. All crystallizations were performed at 293 K.

2.3. Data collection and processing

All crystals of *sto*PCNA2–*sto*PCNA3 were transferred into a cryoprotectant solution composed of reservoir solution containing 40% (v/v) glycerol and flash-cooled in a nitrogen stream at 100 K. Two sets of diffraction data were collected from crystals which belonged to different space groups. Diffraction data from a crystal belonging to space group *I*222 were collected on a MicroMax 007 generator with

an R-AXIS IV⁺⁺ image-plate detector (Rigaku) using an oscillation of 0.5° per frame, an exposure time of 10 min and a crystal-to-detector distance of 230 mm. A total of 540 frames were collected. Diffraction data from a crystal belonging to space group *P*2₁2₁ were collected with a DIP-6040 image-plate detector (MAC Science/Bruker AXS) on SPring-8 beamline BL44XU (Harima, Japan) using an oscillation of 1.0° per frame, an exposure time of 4 s and a crystal-to-detector distance of 500 mm. A total of 180 frames were collected.

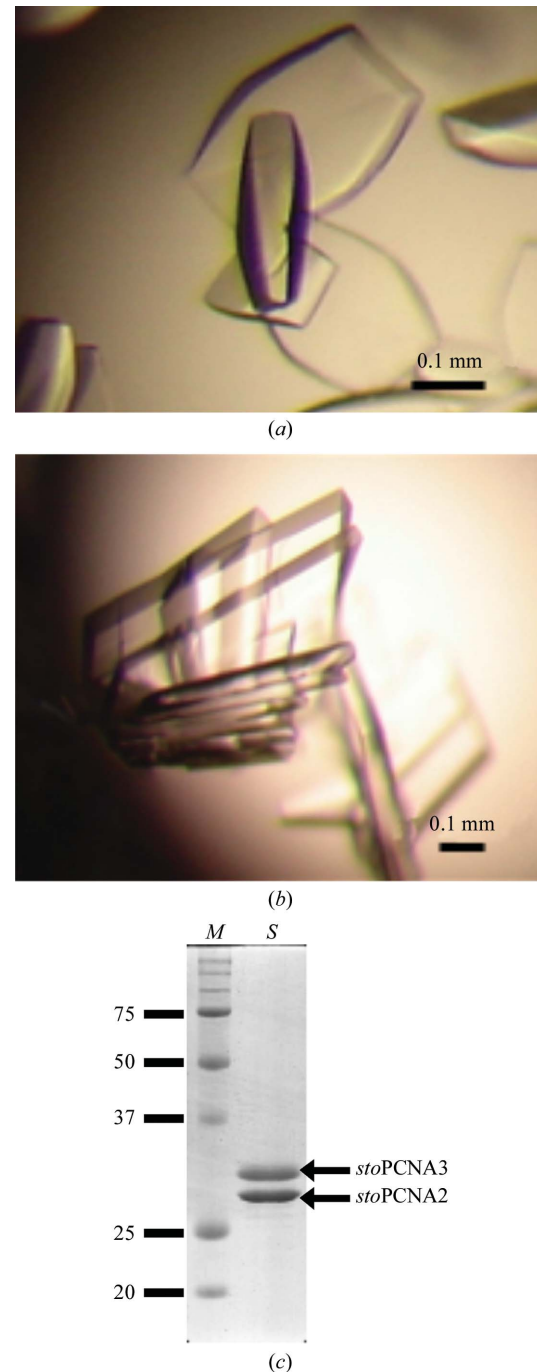


Figure 1

Crystals of the *sto*PCNA2–*sto*PCNA3 complex. (a) Crystals of the *sto*PCNA2–*sto*PCNA3 complex with dimensions of 0.03 × 0.1 × 0.3 mm obtained using condition A. (b) Crystals of the *sto*PCNA2–*sto*PCNA3 complex with dimensions of 0.05 × 0.8 × 1.0 mm obtained using condition B. (c) SDS–PAGE analysis of the crystals obtained using condition A. Lane M, molecular-mass markers (kDa); lane S, crystals.

Table 1

Data-collection and processing statistics.

Values in parentheses are for the highest resolution shell.

Space group	<i>I</i> 222	<i>P</i> 2 ₁ 2 ₁ 2
Source	MicroMax 007	SPRING-8 BL44XU
Wavelength (Å)	1.5418	0.9000
Unit-cell parameters (Å)	<i>a</i> = 91.1, <i>b</i> = 111.8, <i>c</i> = 170.9	<i>a</i> = 91.1, <i>b</i> = 160.6, <i>c</i> = 116.6
Resolution range (Å)	50.0–2.90 (3.06–2.90)	50.0–2.80 (2.95–2.80)
No. of observed reflections	211300 (30521)	297177 (43300)
No. of unique reflections	19736 (2830)	42314 (6051)
Redundancy	10.7 (10.8)	7.0 (7.2)
Completeness (%)	100 (100)	98.9 (97.6)
<i>R</i> _{merge} [†] (%)	10.1 (49.5)	13.5 (44.9)
<i>R</i> _{r.i.m.} [‡] (%)	10.5 (51.8)	14.6 (48.3)
<i>R</i> _{p.i.m.} [§] (%)	3.1 (15.1)	5.5 (17.7)
$\langle I/\sigma(I) \rangle$	19.7 (5.4)	10.3 (4.5)
No. of protein molecules in ASU	1 <i>sto</i> PCNA2, 1 <i>sto</i> PCNA3	2 <i>sto</i> PCNA2, 2 <i>sto</i> PCNA3

[†] $R_{\text{merge}} = 100 \times \sum_{hkl} \sum_i |I_i(hkl) - \langle I(hkl) \rangle| / \sum_{hkl} \sum_i I_i(hkl)$. [‡] $R_{\text{r.i.m.}} = 100 \times \sum_{hkl} [N/(N-1)]^{1/2} \sum_i |I_i(hkl) - \langle I(hkl) \rangle| / \sum_{hkl} \sum_i I_i(hkl)$. [§] $R_{\text{p.i.m.}} = 100 \times \sum_{hkl} [1/(N-1)]^{1/2} \sum_i |I_i(hkl) - \langle I(hkl) \rangle| / \sum_{hkl} \sum_i I_i(hkl)$. $\langle I(hkl) \rangle$ is the mean value of $I(hkl)$ and N is the redundancy.

All diffraction data sets were processed, integrated and scaled with *iMOSFLM* (Leslie, 1992) and *SCALA* (Evans, 1997) from the CCP4 program suite (Collaborative Computational Project, Number 4, 1994).

3. Results and discussion

Thin crystals of *sto*PCNA2–*sto*PCNA3 appeared from several crystallization conditions in the initial crystallization screening, in which ammonium sulfate and sodium citrate were common precipitants. To increase the thicknesses of the crystals, the crystallization conditions were optimized using 20–40 mg ml⁻¹ protein and reservoir solutions with various pH values, precipitant concentrations and additives. The total number of optimization droplets was approximately 2000. Plate-like crystals appeared after 1–2 weeks using two crystallization conditions: 20 mg ml⁻¹ protein, 1.6 M ammonium sulfate, 0.1 M sodium acetate pH 5.0 (condition *A*; Fig. 1a) and 20 mg ml⁻¹ protein, 0.2 M sodium citrate, 18% (w/v) polyethylene glycol 3350, 0.1 M HEPES pH 7.0 (condition *B*; Fig. 1b). X-ray diffraction was not detected from the crystals obtained using condition *B*, but was clearly observed from those obtained using condition *A*. SDS-PAGE analysis of the latter crystals revealed that they contained the *sto*PCNA2–*sto*PCNA3 complex (Fig. 1c).

Two crystal forms were obtained using condition *A*. One crystal form belonged to the *I*-centred orthorhombic space group *I*222, with unit-cell parameters *a* = 91.1, *b* = 111.8, *c* = 170.9 Å. The other crystal form belonged to the primitive orthorhombic space group *P*2₁2₁2, with unit-cell parameters *a* = 91.1, *b* = 160.6, *c* = 116.6 Å. Table 1 summarizes the data-collection statistics.

Molecular-replacement searches using diffraction data from the *I*222 form were carried out for both *sto*PCNA2 and *sto*PCNA3 using

the coordinates of *sso*PCNA (51% and 53% sequence identity to *sto*PCNA2 and *sto*PCNA3, respectively; PDB code 2izo; Doré *et al.*, 2006) as search models. Calculations were performed with *Phaser* (McCoy *et al.*, 2007) from the CCP4 suite. A search for *sto*PCNA3 was first performed and one clear solution (LLG = 404, *Z* score = 19.2) was obtained. Fixing the solution for *sto*PCNA3, a search for *sto*PCNA2 was conducted and an initial model with a good score (LLG = 964, *Z* score = 26.4) was obtained. Although a trimeric structure consisting of one *sto*PCNA2 molecule and two *sto*PCNA3 molecules was expected (Lu *et al.*, 2008), the initial model showed the presence of only one *sto*PCNA2 and one *sto*PCNA3 molecule in the asymmetric unit and the model generated by symmetry operations suggested a tetrameric ring-like structure consisting of two *sto*PCNA2 and two *sto*PCNA3 molecules. The models generated from the diffraction data of *P*2₁2₁2 form also indicated tetrameric structures. According to Matthews coefficient calculations (Matthews, 1968), the crystals belonged to space groups *I*222 and *P*2₁2₁2, with Matthews coefficients *V*_M of 3.96 and 3.90 Å³ Da⁻¹, respectively. Precise model building and structure refinements are currently being performed.

We are grateful to Dr Eiki Yamashita, Professor Atsushi Nakagawa and the beamline staff for their support at SPring-8 BL44XU. This work was partly supported by the National Project on Protein Structural and Functional Analysis by the Ministry of Education, Culture, Sports, Science and Technology of Japan (Protein 3000 project). We thank Professor Seiki Kuramitsu for organizing the research group in the program.

References

- Collaborative Computational Project, Number 4 (1994). *Acta Cryst. D* **50**, 760–763.
- Dionne, I., Nookala, R. K., Jackson, S. P., Doherty, A. J. & Bell, S. D. (2003). *Mol. Cell.* **11**, 275–282.
- Doré, A. S., Kilkenny, M. L., Jones, S. A., Oliver, A. W., Roe, S. M., Bell, S. D. & Pearl, L. H. (2006). *Nucleic Acids Res.* **34**, 4515–4526.
- Evans, P. R. (1997). *Int CCP4/ESF-EACBM Newslett. Protein Crystallogr.* **33**, 22–24.
- Gulbis, J. M., Kelman, Z., Hurwitz, J., O'Donnell, M. & Kuriyan, J. (1996). *Cell*, **87**, 297–306.
- Imamura, K., Fukunaga, K., Kawarabayashi, Y. & Ishino, Y. (2007). *Mol. Microbiol.* **64**, 308–318.
- Kong, X. P., Onrust, R., O'Donnell, M. & Kuriyan, J. (1992). *Cell*, **69**, 425–437.
- Krishna, T. S., Kong, X. P., Gary, S., Burgers, P. M. & Kuriyan, J. (1994). *Cell*, **79**, 1233–1243.
- Leslie, A. G. W. (1992). *Int CCP4/ESF-EACBM Newslett. Protein Crystallogr.* **26**.
- Lu, S., Li, Z., Wang, Z., Ma, X., Sheng, D., Ni, J. & Shen, Y. (2008). *Biochem. Biophys. Res. Commun.* **346**, 269–374.
- Matsumiya, S., Ishino, Y. & Morikawa, K. (2001). *Protein Sci.* **10**, 17–23.
- Matthews, B. W. (1968). *J. Mol. Biol.* **33**, 491–497.
- McCoy, A. J., Grosse-Kunstleve, R. W., Adams, P. D., Winn, M. D., Storoni, L. C. & Read, R. J. (2007). *J. Appl. Cryst.* **40**, 658–674.
- Moldovan, G. L., Pfander, B. & Jentsch, S. (2007). *Cell*, **129**, 665–679.
- Williams, G. J., Johnson, K., Rudolf, J., McMahon, S. A., Carter, L., Oke, M., Liu, H., Taylor, G. L., White, M. F. & Naismith, J. H. (2006). *Acta Cryst. F* **62**, 944–948.